PEDOSPHERE（土壤圈英文版）

Pedosphere ISSN 1020-0160/CN 32-1315/P 10.1016/S1002-0160(21)60050-4

Running Title: ROCK-EVAL® ANALYSIS OF SOIL SIZE-FRACTIONS

Size-fractions of Organic Matter Pools Influence their Stability: Applying Rock-Eval® Analysis to Beech Forest Soils

David SEBAG[1,2,3], Eric P. VERRECCHIA[2], Thierry ADATTE[4], Michaël AUBERT[5], Guillaume CAILLEAU[6], Thibaud DECAËNS[7], Isabelle KOWALEWSKI[3], Jean TRAP[8], Fabrice BUREAU[5+], Mickaël HEDDE[8+]

[1] *Normandie Univ, UNIROUEN, CNRS, M2C, 76000 Rouen (France)*

[2] *Institute of Earth Surface Dynamics, IDYST, Geopolis, University of Lausanne, Lausanne (Switzerland)*

[3] *IFP Energies Nouvelles, Geosciences Division, 92852 Rueil-Malmaison (France)*

[4] *Institute of Earth Sciences, ISTE, Geopolis, University of Lausanne, Lausanne (Switzerland)*

[5] *Normandie Univ, UNIROUEN, IRSTEA, ECODIV, 76000 Rouen (France)*

[6] *Laboratory of Microbiology, Institute of Biology, University of Neuchâtel, Neuchâtel (Switzerland)*

[7] *Université de Montpellier, CNRS, CEFE, Montpellier (France)*

[8] *Eco&Sols, INRA, IRD, Université de Montpellier (France)*

[+] *co-last authorship*

(Received , 20???; revised , 20???)

ABSTRACT

Soil organic matter (OM) is a complex heterogeneous mixture: resulting from decomposition and organo-mineral interactions, it challenges characterization in terms of composition and biogeochemical stability. From this perspective, the Rock-Eval® method is a rapid and efficient thermal analysis, which combines quantitative and qualitative information on soil OM, including several parameters related to thermal stability. This approach has already been used to monitor changes in OM properties at landscape, cropland, and profile scales. This study aims to assess the stability of soil organic matter pools by characterizing grain-size fractions from forest litters and topsoils using Rock-Eval® thermal analyses. Organic and topsoil samples were selected from a beech forest located in Normandy (France), whose management has been documented for the last 200 years. Fractionation by wet sieving was used to separate large debris (>2000 µm), coarse (200–2000 µm), and fine particulate organic matter (50–200 µm) in organic samples, and coarse (200–2000 µm), medium (50–200 µm), and fine (<50 µm) fractions in topsoils. Rock-Eval® was able to provide thermal parameters sensitive enough to study fine-scale soil processes. In organic layers, quantitative and qualitative changes are all explained by progressive decomposition of labile organic compounds from plant debris to the finest organic particles. On the other hand, the grain size fractions of the topsoil display different characteristics: indeed, the coarse organo-mineral fractions show high C contents, but with a different composition and a higher thermal stability and degree of decomposition than the plant debris forming the organic layers. These results are consistent with previous studies concluding that the microbial activity is more effective in this fraction. The finest fractions of topsoil reveal low C contents and the highest thermal stability, but also a low degree of decomposition, which can be explained by stronger interactions with the mineral matrix. Therefore, it is suggested that the dynamics of OM present in the different size fractions be interpreted in the light of a plant-microbes-soil continuum. Finally, three distinct thermal stability C pools are highlighted through the grain-size heterogeneity of soil OM: free-coarse organic matter (large debris, coarse and fine particles), weakly-protected organic matter in (bio)aggregates (coarse fraction of topsoil), and stabilized organic matter in fine fractions of topsoil, the latter resulting from interactions inside organo-mineral complexes. These results allow Rock-Eval® thermal parameters to be used in order to empirically illustrate the conceptual models emphasizing the role of drivers played by the gradual decomposition and protection of the most thermally labile organic constituents.

Key Words: aggregates, decomposition, organo-mineral interaction, plant-microbe-soil continuum, soil organic matter, stabilization, thermal analysis

Citation：Sebag D, Verrecchia E P , Adatte T, Aubert M, Cailleau G, Decaëns T, Kowalewski I, Trap J, Bureau F, Hedde M. 2???. Size-fractions of organic matter pools influence their stability: applying Rock-Eval® analysis to Beech forest soils. Pedosphere. 2???(???): ???--???.

INTRODUCTION

Thermal analysis techniques are frequently used to quantify the thermal stability of soil organic matter (OM). In addition to various compositional parameters, this approach can be seen as a proxy of the biogeochemical stability defined as the bioavailability (or bioaccessibility) of soil OM to decomposition by microorganisms (e.g., Plante *et al.*, 2009). The literature dealing with this topic is plentiful and different research schools are still debating the relationships between “analytical” thermal stability and “functional” biogeochemical stability. Many studies investigated thermograms as proxies of soil OM stability (e.g., Plante *et al.*, 2011; Peltre *et al.*, 2013), but the question is still being debated regarding the thermal oxidation of soil OM. Criticisms particularly focused on the accuracy of oxidative thermal analyses (i.e., combustion), which poorly discriminate for biological recalcitrance and are sensitive to C contents (e.g., Peltre *et al.*, 2013; Schiedung *et al.*, 2017). Nevertheless, as Gregorich *et al.* (2015) noted about the Rock-Eval® analytical process, it *“is fundamentally different than other thermal degradation techniques in that it involves use of an inert atmosphere and rapid heating rates, and because it characterizes the reaction products from heating rather than properties of the bulk sample”*.

Some studies have been initiated to calibrate the results obtained by Rock-Eval® analysis in association with conventional techniques (e.g. Carrie *et al.*, 2012; Delarue *et al.*, 2013; Hare *et al.*, 2014). For example, comparing Rock-Eval® parameters and direct information on structural and conformational characteristics (^{13}C-CPMAS-NMR), Albrecht *et al.* (2015) concluded that the precision of Rock-Eval® parameters is good enough to identify thresholds in OM quality and thermal stability induced by microbial community changes. Coupling Rock-Eval® analysis with a XANES spectroscopic technique, Gregorich *et al.* (2015) showed that the loss of soil OM generally involved preferential degradation of H-rich compounds. In the same way, Barré *et al.* (2016) demonstrated that persistent soil OM is thermally more stable and has less hydrogen-rich compounds (low Hydrogen Index) than labile soil OM thanks to a combination of thermal analysis, differential scanning calorimetry, and evolved gas analysis (DSC/EGA). Finally, Soucémarianadin *et al.* (2018) showed that Rock-Eval® parameters were good estimates of the labile C pool in soils identified by biological or physical approaches (i.e., soil respiration test and particulate organic matter isolated by a physical fractionation).

At higher scales, some studies focus on functional compartments, i.e. the coarse and fine free particulate OM (cPOM, fPOM) as well as the mineral associated OM (MAOM) fractions. The former usually display a low thermostability, corresponding to the most labile C pools, while the latter exhibits a high thermostability, i.e. a more stable C pool (Saenger *et al.*, 2013, 2015; Gregorich *et al.*, 2015). The literature mainly emphasizes the role of OM stability on C sequestration in soils, as controlled by environmental drivers (plant cover, land use, climate). But some studies open other perspectives. For instance, Sebag *et al.* (2016) illustrated the relevance of two combined thermal indices derived from the pyrolytic step of Rock-Eval® analysis to study the dynamics of more reactive fraction of soil OM (i.e., pyrolysable carbon). Indeed, these thermal indices are, by construction, highly correlated if the stabilization processes are driven by the gradual decomposition of thermally labile fractions (Albrecht *et al.*, 2015; Sebag *et al.*, 2016; Matteodo *et al.*, 2018; Thoumazeau *et al.*, 2020). This relationship is especially observed in OM-rich samples and interpreted as a consequence of the progressive decomposition of particulate OM (POM) as described by Lehmann and Kleber (2015). On the other hand, OM-poor samples, and some soil classes (e.g., Podzols, Arenosols), display a deviation from this relationship, reflecting the interactions between organic fraction and the mineral matrix (Saenger *et al.*, 2015; Sebag *et al.*, 2016; Matteodo *et al.*, 2018; Malou *et al.*, 2020).

This body of knowledge supports the hypothesis that I/R diagram integrates (1) the intrinsic stability (or biological recalcitrance) of OM (i.e., the energy input to break down organic molecules), as well as (2), the stabilization of soil OM through interactions with soil minerals (i.e., the energy required to break the bonding of soil OM with mineral particles). Consequently, we tested this hypothesis by characterizing the Rock-Eval® signatures (organic carbon content, compositional and thermal indices) of bulk samples and size fractions of organic layers and topsoils from a beech forest. More precisely, we monitored the evolution of their thermal status that is supposed to describe a continuum from the most labile forms in organic layers (biogenic precursors) to the most stable forms in subsoils.

MATERIAL & METHODS

Site settings and previous studies

The study site is located in the Eawy State Forest (France, Normandy, 01°18'E; 49°44'N; 7200 ha) whose management has been documented for 200 years. The climate is oceanic temperate with a mean annual temperature of 10°C and 800 mm of mean annual precipitation. The soil is an endogleyic dystric Luvisol (FAO, 2006) developed on a > 80 cm thick layer of loess (silty texture), overlying clay-with-flint parent material. Soil texture was similar among stands, with 13% of clay, 70% of silt, and 17% of sand. The understory vegetation is a characteristic *Endymio-Fagetum*, according to the phytosociological classification (Durin *et al.*, 1967).

A set of research studies has been performed over a period of 10 years about both soil biota (microorganisms, mesofauna, and macrofauna; Aubert *et al.* 2003b; Hedde *et al.* 2007; Chauvat *et al.* 2011; Trap *et al.* 2011c) and soil OM dynamics (litter decomposition, N cycling, soil C stock; Aubert *et al.* 2004, 2006, 2010; Hedde *et al.* 2008; 2010; Trap *et al.* 2011ab). The main outputs of these studies are summarized in the review by Aubert *et al.* (2018). Over a 200-yr chronosequence, it has been shown that the best performance of the forest ecosystem, defined as a high organic matter recycling system, is achieved when plant and soil communities jointly exhibit limiting similarity and complementarity in species functional traits. However, soil and humus C fractions were studied in terms of mass, content, and stock dynamics but their stability is still deserving further assessment.

Sampling

The studied sample set (Table 1) originates from previous studies on soil OM dynamics (i.e., quantitative and qualitative changes) and combines morphological description, physical fractionation, and C and N determinations (Hedde *et al.*, 2008). The selected plots cover the whole silvicultural cycle (over a period of 200 years). Plots have always been occupied by the same tree species (*Fagus sylvatica L.*) minimizing possible changes in the chemical composition of plant debris.

The humipedon (i.e., the upper part of a soil constituted by organic and/or organo-mineral horizons, Zanella *et al.* 2018) was described in 15 stands with five points per stand within a 25 cm x 25 cm quadrat, leading to a total of 75 humipedon. Each humipedon was separated into OL, OF/OH, and A horizons, according to macroscopic morphological characteristics (Jabiol *et al.*, 2007). This horizon nomenclature corresponds to the USDA nomenclature as follows: OL equals Oi, OF equals Oe, and OH equals Oa. Afterwards, horizons were sampled on the delimited area, stored in plastic bags, and weighed after air-drying in the laboratory.

Fractionation

The physical fractionations were performed on OF/OH horizons and topsoils with a method depending on the nature of the samples (Hedde *et al.*, 2008).

We assume that the state of decomposition of particulate OM in organic layers is a function of its particle size as decay induces fragmentation. In OF/OH samples, logs, herbaceous vegetation litter, and beech fruits (masts and nuts) were separated from remaining organic material (rOM) and weighed. Then, the size distribution of the rOM was assessed by wet sieving using a vibratory sieve shaker. rOM was moistened in deionised water, deposited on the top sieve, and sieved on 2000, 200 and 50 μm meshes. These fractions were subjected to flotation-panning in water to separate a light fraction, consisting of light OM, from a heavy fraction, consisting mainly of mineral material. Fractions were oven-dried (40 °C for 48 h) and weighed. The finest mineral fraction (<50 μm) has been excluded. The resulting light organic fractions (O-fractions) were decaying beech leaves (large debris, >2000 μm), coarse particulate organic matter (O-coarse, 200–2000 μm), and fine particulate organic matter (O-medium, 50–200 μm). These latter two O-fractions are finally comparable to the functional litter compartments O-cPOM and O-fPOM, respectively.

On the other hand, subsamples of air-dried topsoil (bulk A) were submitted to physical dispersion of particles prior to fractionation as described by Balesdent *et al.* (1991). Soil samples were shaken with glass beads on an end-over-end shaker for 16 h. The dispersed fractions were then separated at 2000, 200, and 50 μm by wet sieving. The coarsest fraction (>2000 μm) was very limited in the studied soils as they developed from loess parent material; therefore, this fraction has been removed. In the remaining fractions, light particulate organic matter was separated from heavier minerals by flotation-sedimentation in water. The <50 μm suspension was flocculated with $CaCl_2$. All the fractions were oven-dried and weighed. The obtained organo-mineral fractions (the A-fractions) were the following: an A-coarse fraction (200–2000 μm), an A-medium fraction (50–200 μm), and an A-fine fraction (<50 μm). These A-fractions do not match exactly with functional soil compartments conventionally referred to as coarse, fine, and occluded particulate OM (cPOM, fPOM, and oPOM) and mineral-associated OM (MAOM). Nevertheless, an examination with a binocular microscope allowed to confirm that the A-coarse fraction was mostly constituted of particulate OM, whereas the A-fine fraction was extremely poor in it. Consequently, A-coarse and A-fine fractions can be reasonably considered as relatively enriched in POM and MAOM, respectively, whereas the A-medium fraction can probably be considered as a composite fraction.

Rock-Eval® thermal analysis

Analyses were carried out with 30 to 70 mg of powdered samples using a Rock-Eval® 6 manufactured by Vinci Technologies. All the device's analytical processes and protocols applied in our study are detailed in the literature (e.g., Lafargue *et al.*, 1998; Behar *et al.*, 2001; Disnar *et al.*, 2003; Sebag *et al.* 2016). Rock-Eval® analysis method is based on continuous measurement of gas effluents (HC - hydrocarbon, CO and CO_2) released during the thermal cracking of organic compounds (and thermal decomposition of carbonate minerals) in pyrolytic conditions (from 200 °C to 650 °C by 25 °C/min steps on an inert atmosphere), then during the combustion of residual carbon (from 300 °C to 850 °C on an oxidative atmosphere). The resulting thermograms are used to calculate standard parameters by integrating the amounts of HC, CO, and CO_2 between defined temperature limits (details in Lafargue *et al.*, 1998; Behar *et al.*, 2001).

Over the last fifteen years, applications to environmental sciences allow OM quality changes to be measured in soils and recent sediments, and C fluxes and stocks to be quantified in various environments. These studies were usually based on the following four standard parameters. The Total Organic Carbon (TOC in percentage by weight) results from a calculation based on the sum of all the C effluents (HC, CO, and CO_2). In soil samples, TOC measures the amount of organic C (in g C per 100g of sample) and was well calibrated in previous studies (e.g., Disnar *et al.*, 2003; Saenger *et al.*, 2013; Malou *et al.*, 2020). The maximum cracking temperature (TpS2 in °C) corresponds to the oven temperature related to the maximum of HC release during pyrolysis. The Hydrogen Index (HI in mg HC. g^{-1} TOC) corresponds to the amount of hydrocarbon released during pyrolysis and relative to TOC.

In soil samples, decreasing HI along the soil profiles are related to deshydrogenation of organic compounds during pedogenesis (e.g., Disnar *et al.*, 2003; Barré *et al.* 2016). The Oxygen Index (OI in mg $CO_2.g^{-1}$ TOC) corresponds to the amount of oxygen released during pyrolysis before 400 °C for CO and 500 °C for CO_2 (i.e., from cracking of organic compounds, not from thermal decomposition of carbonate) and relative to TOC. In soil samples, increasing OI along the soil profiles is related to a relative oxygenation often interpreted as an aromatization of organic compounds.

In addition to these standard parameters, Disnar *et al.* (2003) proposed to use the shape of thermograms in order to get additional information about SOM quality. In this study, we used R-index (R) to measure the contribution of resistant and refractory C pools, and the I-index (I) to quantify the preservation of the labile C pool (Sebag et al 2016). Both indices are derived from integrated S2 areas between specific bounds (200-400 °C, 400-460 °C, and above 460 °C), usually interpreted as specific thresholds in thermal stability of organic compounds, separating thermally labile, resistant, and refractory C pools (fig. SM1 and SM2; Disnar *et al.*, 2003; Sebag *et al.*, 2006; Saenger *et al.*, 2013, 2015). Both indices are calculated from S2 thermograms (i.e., hydrocarbon compound released by thermal cracking under pyrolytic conditions) that seem little or not sensitive to interference with mineral matrix and catalytic reactions. They were therefore developed to study the most reactive fraction of soil OM (i.e., richer in H-bond and thermally labile), which is directly involved in short-term changes of soil carbon dynamics. Nevertheless, as recommended by Schiedung *et al.* (2017), these thermal indices do not consider the various labile pools, i.e., they do not reflect biological stability, but focus on soil OM biogeochemical stability.

RESULTS

Standard Rock-Eval® parameters

TOC values vary in bulk samples (42 to 55% in OL; 3 to 8% in A; Table 1), in OF/OH-fractions (> 41% in large debris, 34 to 56% in O-coarse, and 21 to 60% in O-medium), and in the A-fractions (38 to 74% in A-coarse, 19 to 40% in A-medium~~,~~ and 1.5 to 6% in A-fine). Boxplots emphasize a fairly continuous decreasing trend from OL (only beech litter) and large debris towards O-fraction and A-coarse with a drastic decreasing shift towards A medium and fine fractions (Fig. 1).

Table 1: Statistical values (1st quartile, median, 3rd quartile) of the measured and calculated Rock-Eval® parameters given in the text, for O and A horizons and their respective fraction sizes.

Fig. 1

Fig. 1. Soil Organic Carbon (SOC %wt) contents of organic horizons (OL litters, OF/OH fractions) and organo-mineral horizons (A-fractions, A horizon). Horizontal bands highlight the range of values from Sebag *et al.* (2016)'s dataset for both bulk samples of litters (green) and topsoils (brown), respectively.

The maximum cracking temperature (TpS2) exhibits the usual pattern, i.e. low values (about 370 °C) for OL horizons and O-fractions, and higher values (420 to 470 °C) for A-fractions and bulk A (Fig. 2A-B).

Fig. 2

Fig. 2. Boxplots of standard Rock-Eval® parameters for the various fraction sizes: on the left-hand side, holorganic horizons (O); on the right-hand side, organo-mineral horizons (A). A-B. Temperatures corresponding to the maximum release of hydrocarbon effluents. C-D. Hydrogen Index (mg HC/g Corg). E-F Oxygen Index (mg CO_2/g Corg).

The Hydrogen Index (HI) has more variable values (Fig. 2C-D). Indeed, OL samples, large debris and coarse fraction of OF/OH horizons display low HI variability, being comprised between 225 and

330 mg HC/g C_{org} (275 mg HC/g C_{org} on average), while medium fractions of OF/OH horizons vary in a wider range: from 240 to 420 mg HC/g C_{org} (340 mg HC/g C_{org} on average). On the other hand, the HI values and their dispersion are strongly higher in all A-fractions (290 to 900 mg HC/g C_{org}), but decrease from the A-coarse (610 mg HC/g C_{org} on average) to A-medium (555 mg HC/g C_{org} on average) and A-fine~~-~~one (455 mg HC/g C_{org} on average), and are quite similar to O-fraction in topsoils (bulk A; 255 to 330 mg HC/g C_{org}).

The Oxygen Index (OI) shows different patterns according to the horizons (Fig. 2E-F). On one hand, OI distribution is particularly remarkable in O-fractions (Fig. 2E). In each fraction, the majority of samples has a low OI ranging from 75 to 150 mg O_2/g C_{org} (median $\approx$ 120 mg O_2/g C_{org}). However, the OI dispersion increases with the decreasing fraction size, with a range from 75 to 250 mg O_2/g C_{org} in O-medium. On the other hand, the OI values and dispersion increase from the A-coarse (about 35 to 340 mg O_2/g C_{org}) up to A-fine (75 to 480 mg O_2/g C_{org}) but decrease in topsoils (bulk A ; 135 to 175 mg O_2/g C_{org}; Fig. 2D).

I/R Diagram

The I/R diagram (Fig. 3) displays a drastic contrast and a large hiatus between litter (OL horizons; high I > 0.9; low R < 0.4) and topsoil (bulk A; low I < 0.5; high R > 0.5), with the O-fractions (OF/OH horizons) distributed along the regression line identified as the “decomposition line” by Sebag *et al.* (2016). The A-fractions are distributed around the topsoil samples (A). The A-medium are distributed along the ”decomposition line”, the A-fine above, and the A-coarse below (Fig. 3A). The R-index ranges of A-coarse and A-medium fractions are close (Fig. 3), highlighting a relatively low I-index of coarse organic constituents (>200 µm). Conversely, the I-index ranges of A-fine and A-medium are closed (Fig. 3), highlighting a relative high R-index of fine organic constituents (<50µm).

Fig. 3

Fig. 3. SOC thermal stability (R-index) and preservation of thermolabile pool (I-index). A. I/R diagram for litters (OL), topsoil (A), and grain-size fractions. Horizontal bands highlight the range of values from Sebag *et al.* (2016)’s dataset for both bulk samples of litters (green) and topsoils (brown), respectively. The central regression line represents the “decomposition line” calculated using the Sebag *et al.* (2016)’s dataset (dotted line refers to the 95% confidence interval). The two other regressions refer to the A-coarse fraction (bottom lines) and the A-fine fraction (upper lines). B. Range of R-index values for A-fractions and topsoil. C. Range of I-index values for A-fractions and topsoil.

DISCUSSION

Rock-Eval® parameters and composition of SOM

The standard Rock-Eval® parameters (TOC, TpS2, HI, OI) refer to general trends and signatures (Figs. 1-2, Tab. 1) related to decomposition and changes in chemical composition of soil OM. The results are in agreement with previous Rock-Eval® studies (e.g., Di-Giovanni *et al.*, 1998; Disnar *et al.*, 2003; Sebag *et al.*, 2006, 2016; Saenger *et al.*, 2013).

The TOC (Fig. 1) decreases continuously from large debris to A-medium fractions, and then drops in the A-fine ones. Hedde *et al.* (2008) already underlined this trend in the studied soils, and explained these changes by a loss of C-based compounds by leaching or microbial decaying. Consequently, in topsoils (bulk A), this trend indicates that the proportion of the mineral matrix increases with the decreasing grain size of the fractions, up to 80% in the finest A-fine. These quantitative results (i.e., C contents) confirm that the fractionation protocol (i.e., sieving and flotation in water) separated a coarse fraction (A-coarse) enriched in OM and a fine fraction (A-fine) enriched in a mineral fraction. In addition, relative contributions indicate that certain fractions are the predominant ones in the samples:

organic layers are mainly composed of large debris (>2mm; 60-70% of C mass), while topsoils are substantially composed of A-fine (32-45% of C mass) (re-calculated from Hedde *et al.* 2008).

The TpS2, HI, OI show that litter (OL horizons) display a homogeneous typical signature of fresh plant tissues falling into the range described by Sebag *et al.* (2016) (TpS2 ≈ 370 °C; HI ≈ 250-300 mg HC/g C_{org}; OI ≈ 120 mg O_2/g C_{org}), which also characterizes OF/OH fractions (large debris and O-coarse). Compared to fresh plant remains, these qualitative results (i.e., OM quality) reflect a low decomposition, with no real impact on the bulk composition of biogenic inputs (i.e., plant tissue).

Similarly to litter, topsoils (bulk A) display values in the order of magnitude of topsoils reported by Sebag *et al.* (2016) (TpS2 ≈ 440-460 °C; HI ≈ 260-400 mg HC/g C_{org}; OI ≈ 150-250 mg O_2/g C_{org}). On the other hand, unlike homogeneous O-fractions, A-fractions exhibit different signatures. The stepwise increase in the TpS2 reflects an increase in thermal stability with decreasing grain-size. This trend, related to decreasing HI and increasing OI values, can be interpreted as a consequence of decomposition, in continuation with the processes occurring in the surficial organic layers. However, very high HI and very low OI of the A-coarse fraction indicate a drastic compositional change compared to O-fractions. Such a change should be related to microbial OM whose biogenic precursors are H-rich and O-poor. These conclusions are corroborated by patterns of C-N ratios. On the same samples, Hedde *et al.* (2008) found maximum values (ca. 27) in OL horizon, with a C-N ratio regularly decreasing with size in O-fractions (23-24, 19-20 and 16-18 in large debris, coarse, and fine fractions, respectively). However, values in A-coarse fraction were 20-22, thus between values reported for O-large and O-coarse fractions.

In this perspective, the fractionation protocol (i.e., sieving and flotation in water) could have separated the following fractions: (1) homogenous O-fractions, constituted by coarse and fine free OM corresponding to fragmented but weakly decomposed (high HI, low TpS2) plant debris (i.e., primary production), (2) an organic coarse A-fraction enriched in weakly decomposed (very high HI) microbial OM (i.e., secondary production), (3) an A-fine fraction enriched in soil minerals and stabilized OM (high TpS2), and (4) an A-medium fraction, intermediate between coarse and fine A-fractions, confirming its composite nature. Finally, these results well illustrate the concept of the "*plant-microbe-soil continuum*". However, the compositional indices (HI, OI) appear, on the one hand, insufficiently sensitive to measure the progressive decomposition of plant debris in the litter, and on the other hand, too sensitive to the composition changes, in order to compare organic fractions to topsoil ones. It is therefore difficult to distinguish between the various processes (i.e., composition of biogenic precursors, decomposition of labile pools, organo-mineral interactions) that may explain the changes in thermal stability measured by TpS2.

Thermal stability and gradual decomposition

When considering the I/R diagram (Fig. 3), results show a pattern of soil OM displaying quality (I-index as decomposition of labile pool) and thermal stability (R-index as contribution of stable pools), in function of the grain-size fractions. High continuous input of organic matter was observed on all the stands using measurement of litter production (Trap *et al.*, 2011). As expected, organic layers (low decomposition, low stability) differ drastically from topsoils (high decomposition, high stability). The hiatus between litters and topsoils also exists between O- and A-fractions and therefore reflects a major threshold. Considering that thermal stability can integrate several mechanisms of OM stabilization (Saenger *et al.*, 2013; Gregorich *et al.*, 2015; Sebag *et al.* 2016), we assume that this gap is probably related to multiple interactions between organic fractions and the mineral matrix.

As expected, all fractions from organic layers (i.e., large debris, O-coarse and O-medium) derive directly from aerial litters that first enter the soil by accumulating in a OL horizon. However, they display an increasing decomposition (i.e., I-index score) and thermal stability (i.e., R-index score). First, both indices of the bulk litter and O-fractions are strongly correlated. In organic samples, this indicates that gradual decomposition of labile pools (decreasing I-index score) is a major driver of OM stabilization (increasing R-index score; Albrecht *et al.* 2015; Matteodo *et al.* 2018; Thoumazeau *et al.*, 2020). Second, O-fractions overlap each other, indicating that evolution processes (i.e., gradual decomposition of labile pools) are probably fairly continuous and comparable for all fractions. Third, variances of both indices are large for all O-fractions, which can be explained by the different ages of the studied plots. Indeed, large debris and O-coarse fractions show a low variability for each stand, but large variations during the sylvicultural cycle (Trap *et al.*, 2011a). On the other hand, O-medium fractions show a relative stability along the 200 yr-chronosequence. These results extend the conclusions of previous studies using the same sample set, which showed that the modification in soil biota activity may be responsible for changes in the decaying processes and SOM dynamics (Hedde *et al.*, 2008; Trap *et al.*, 2013). Thermal analysis shows that the stability of the coarser fractions in organic layers (large debris and O-coarse) could be affected by temporal changes in soil biota activity (Trap *et al.*, 2011c), whereas the stability of the finer fractions (O-fine) varies slightly over time. Topsoil and A-medium fractions, is plotted along the "decomposition line" (Fig. 3) meaning that the gradual decomposition of the most labile compounds continues to play a major role in the stabilization of the soil OM. Conversely, the positions of the A-coarse below the "decomposition line", and of the A-fine above it, reveal differences in the stabilization processes. The range of R-index values of A-coarse is comparable to the A-medium, meaning that the stability benefit (positive R shift compared to O-fraction) is in the same order of magnitude for both fractions, and could be related to the physical protection provided by the mineral matrix for all A-fractions. Nevertheless, the lower I-index values of A-coarse reflect a higher decomposition of thermo-labile constituents. One explanation could be based on differences in aggregate sizes for each fraction, knowing that occlusion is more efficient in micro- than in macro-aggregates (e.g., Six *et al.*, 2002). But the structural analysis of these soils demonstrated that they were essentially constituted by micro-aggregates (Trap *et al.*, 2011a). Therefore, another hypothesis would consist into the relationship between thermal status and compositional indices: an advanced decomposition of the most labile fraction (low I-index) coincides with a significant increase in HI. But this relationship is contrary to the evolution of plant debris in litters and soils (i.e. a decreasing HI). On the other hand, the microbial activity could provide interesting clues: I-index values can be influenced by intense microbial decomposition of plant OM, whereas HI values reflect the synthesis of H-rich microbial OM.

Finally, the A-fine fraction presents a higher thermal stability (highest R-index value) than A-medium, but without differences in decomposition of thermo-labile pool (I-index). This can be related to the strong interactions between this finest OM fraction and an abundant mineral matrix: both A-medium and A-fine fractions would be physically protected in micro-aggregates, but the second would also be protected at a finer scale (occlusion within clay microstructures, adsorption on mineral surfaces, and/or formation of organo-mineral complexes).

From this perspective, the I/R diagram emphasizes that the thermal stability (R-index) of topsoil OM continuously due to the gradual decomposition (I-index) of the most labile pools. (i.e. high inverse correlation between both indices on the continuation of the "decomposition line"). In addition, different thermal status can be assigned depending on the type of relationship with the mineral matrix. The organic particles constituting the A-coarse fraction (200-2000 µm) are larger than the topsoil micro-aggregates. They are poorly protected by occlusion and more easily accessible and decomposed by soil microorganisms. The organic particles forming the A-medium fraction (50-200 µm) are better protected in micro-aggregates (occlusion) and would be less bioavailable for soil microorganisms. However, because of the separation protocol, it is not possible to exclude the hypothesis of a composite A-medium fraction with an intermediate signature between two functional compartments (POM and MAOM). The organic constituents of the A-fine fraction (<50 µm) are diluted in an abundant mineral matrix. As they have a higher thermal stability without showing any further decomposition state compared to the A-medium fraction, it is reasonable to assume that this is related to an additional protection provided by the mineral matrix (i.e., occlusion in clay microstructures, adsorption, and/or complexation).

Finally, the main conclusions of this study are summarized in Figure 4, which shows the relationships between the thermal stability indices, the size fractions, the thermal C-pools (labile, resistant, refractory), and some pedogenic processes. The differential mineralization in fractions of organic layers causes the decrease of labile C-pool, and the proportional increase of resistant and refractory ones, resulting in the decrease of the decomposition index (I-index derived from labile/resistant ratio) and the relative increase of stability (R-index derived from resistant+refractory). As the changes in resistant and refractory C-pools are directly resulting from the labile C-pool decrease, this free OM is plotted on the "decomposition line". On the other hand, all A fractions are related to stabilisation processes involving matrix protection. These mechanisms attenuate decomposition processes as, even labile, this protected pool reacts as stable compounds. Consequently, it means that labile C-pool decreases in favour of resistant C-pool, resulting in a proportional shift of the decomposition (lower I) and stability (higher R). The same mechanisms allow the fraction occluded in micro-aggregates (on the "decomposition line") and a weakly protected ~~–~~fraction (below the "decomposition line") to be discriminated. In the same way, the interactions with the soil mineral fraction provides a protection strong enough to increase resistant and refractory pools, resulting in higher stability (above the "decomposition line").

Fig. 4

Fig. 4. Key for I/R diagram interpretation from relationships between thermal stability indices, size fractions, C-pools (labile, resistant, refractory), and some pedogenic processes. L: thermo-labile C pools; Rs: thermo-resistant C-pool; Rf: thermo-refractory C-pool. I : I-index; R: R-index. Colors and arrow sizes refer to the effect of the stabilization process on the indices: decreasing of I-index and concomitant increasing R-index. If the two changes are equivalent, data plot on the "decomposition line"; if the decreasing is higher than the increasing, then data plot below the "decomposition line"; finally, if the increasing is higher than the decreasing, then data plot above the "decomposition line".

SOC stability and SOM dynamics

We consider that changes in OM quality (I-index, HI, OI) and thermal stability (R-Index, TpS2) reflect the consequences of differences ~~-~~in biogeochemical stability of grain-size fractions. Indeed, these results illustrate a conventional model of the biogeochemical stabilization, *i.e.* splitting OM into free and protected pools, the latter being protected in organo-mineral assemblages, (bio)aggregates, and/or clay microstructures (von Lützow *et al.*, 2007). It is straightforward to relate this conventional pool model with the interpretation of the I/R diagram. Indeed, the gap in the decomposition degree (I-index) can be seen as a distinction between the free particulate OM in litters, large debris O-coarse, and O-medium, and the protected OM, which gathers weakly-protected (A-coarse), well- protected (A-medium), and strongly- stabilized OM (A-fine) according to their relative position in the I/R diagram (Fig. 3). In the litter, the different fractions are, by nature, enriched in free particulate OM and are probably rapidly turned over. But, in topsoils, any discussion about residence times remains speculative, as the separation protocol does not isolate pure functional compartments.

However, OM dynamics can be represented schematically by crossing quantitative (C stocks) and qualitative (bulk composition and thermal stability) variables. Because studied soils are comparable, the TOC parameter can be used to represent the relative changes in SOC contents in the various grain-size fractions (Fig. 5). In the organic layers (*i.e.*, litter et OF/OH horizons), OM changes are mainly related to biochemical processes (*i.e.*, progressive decomposition and mineralization of labile compounds) driven by some intrinsic OM properties (such as structural stability of organic compounds) and extrinsic environmental factors (such as primary production, edaphic conditions, and biota). In the topsoils (i.e., bulk A), the differences observed between the various size fractions appear disconnected from the properties of the overlying organic layers, but directly related to their interactions with the mineral matrix (soil structure, mineral surfaces, etc.).

Fig. 5

Fig. 5. Changes in soil organic carbon quantity (TOC in g C per 100g of sample) compared to SOM quality (I-index as a degree of preservation of the thermolabile pool) according the grain-size fractions in relationship with external drivers, biota, and mineral matrix. In the various fractions of O-horizons, the main factor is a mineralization (decreasing TOC) of biological compounds, leading to relative increasing of SOM stability (decreasing I-index) due to preservation of a resistant pool. In the fractions of the A-horizons, stability derives from the interaction between biota and mineral matrix leading to a

higher SOM stability (gap in the I-index) due to the formation of a refractory pool. This change in stability can induce an increase in TOC as a result of sequestration.

Thus, our results can be interpreted within the framework of the emergent view and current debates about soil organic carbon dynamics. As assumed by Schmidt *et al.*'s "*conceptual model*" (2011), the Rock-Eval® analysis emphasizes a clear disconnection between organic and mineral samples (litter/topsoil, organic/mineral fractions) in OM contents, composition, and thermal stability. In addition, changes in compositional parameters (HI, OI) seem to pinpoint the main stages of the "*plant-microbe-soil continuum*" by highlighting (1) the source (i.e., plant remains) of the organic particles in the organic layers, (2) the probable impact of organisms on topsoil coarse fractions, and therefore poorly protected by the micro-aggregates, and (3) the specific signature of the fine fractions that dominates in topsoils. Moreover, the thermal parameters provide an empirical illustration of Lehmann & Klebert's "Soil Continuum Model" (2015). Indeed, the I/R diagram graphically represents (1) the progressive decomposition of the most labile compounds (i.e., "decomposition line"), which starts in the litter and continues down to the finest fractions of the topsoils, and (2) a clustering of the topsoil fractions that can be related to the types of interactions between organic particles and soil minerals. On this point, it features the Williams & Plante's "*bioenergetic framework*" (2018) that utilizes thermally determined activation energy and energy density for assessing the persistence of soil OM. Nevertheless, further studies will be necessary to verify whether thermal pools can be assimilated to functional compartments and whether the R- and I-indices can be related to activation energy and energy density, respectively.

CONCLUSIONS

This study highlights some assets of the Rock-Eval® thermal analysis and its derived parameters, in order to quantify the decomposition and stability of soil OM. The various parameters, i.e. Hydrogen, I-, and R-indices, which are related to the most reactive part of the soil OM, stress the changes in the OM composition and thermal stability induced by the decomposition of labile compounds, as well as the organo-mineral interactions in topsoils.

Moreover, this combination of compositional and thermal indices assumes that, at least three thermal C pools can be identified in order to model the grain-size heterogeneity of soil OM: (i) a free particulate plant-derived OM (weak decomposition, low stability) in the litter and organic layers, (ii) a coarse weakly-protected OM (high decomposition, high stability) probably partly decomposed by microorganisms in organic fractions of topsoils, and (iii) a fine stabilized OM (high decomposition, high stability) related to the mineral fractions of topsoils.

Although they do not correspond exactly to the conventional functional compartments, these thermal pools allow the dynamics of OM to be described in forest soils developed on loess in north-western France. This case study accurately illustrates the concept of the plant-microbe-soil continuum and the new emerging paradigms contributing to a comprehensive understanding of OM formation and its fate in soils. This study clearly recognizes that size and stoichiometry of decomposition products interact with the soil matrix to determine their thermal stability. Further studies should now focus on the evolution of the thermal properties of OM according to the changes in soil (micro)biota over time.

ACKNOWLEDGEMENT(S)

Rock-Eval® is a trademark registered by IFP Energies Nouvelles. Jean Trap's research was funded by the French ''Ministère de l'Agriculture et de la Pêche'', the ''GIP ECOFOR'' (rant No. 82005.20), and the GRR-SER (Environmental Sciences, Analysis and Risk Management). Mickaël Hedde's research was supported by the Haute-Normandie Region (France) in the framework of the GRR-SER, and this specific work, by the FR CNRS 3730 SCALE (ESTER project). The "Fondation Herbette – Université de Lausanne" kindly supported David Sebag during his stays at the University of Lausanne. We thank the staff at the University of Lausanne (Switzerland) for their technical and scientific supports ; we are particularly grateful to Stéphanie Grand (Institute of Earth Surface Dynamics). We thank Alyssa Fischer (University of Neuchâtel) for the R script used in drawing the S2 thermograms. Karin Verrecchia kindly edited the first version of the manuscript. All the authors want to thank two anonymous reviewers for their very constructive remarks that substantially improved the first version of the manuscript.

SUPPLEMENTARY MATERIAL

Supplementary material for this article can be found in the online version.

REFERENCES

Albéric P, Lepiller M. 1998. Oxidation of organic matter in a karstic hydrologic unit supplied through stream sinks (Loiret, France). *Water Research* **32**: 7--2051.

Albrecht R, Sebag D, Verrecchia E. 2015. Organic matter decomposition: bridging the gap between Rock–Eval pyrolysis and chemical characterization (CPMAS 13C NMR). *Biogeochemistry* **122**: 101--111.

Aubert M, Alard D, Bureau F. 2003a. Diversity of plant assemblages in managed temperate forests: a case study in Normandy (France). *Forest Ecology and Management* **175**: 321--337.

Aubert M, Hedde M, Decaëns T, Bureau F, Margerie P, Alard D. 2003b. Effects of tree composition on earthworms and other macro-invertebrates in beech forests of Upper Normandy (France). *Pedobiologia* **47**: 904--612.

Aubert M, Bureau F, Alard D, Bardat J. 2004. Effect of tree mixture on the humic epipedon and vegetation diversity in managed beech forest (Normandy, France). *Canadian Journal of Forest Research* **34**: 233--248.

Aubert M, Margerie P, Ernoult A, Decaens T, Bureau F. 2006. Variability and heterogeneity of humus forms at stand level: Comparison between pure beech and mixed beech-hornbeam forest. *Ann. For. Sci.* **63**: 177--188.

Aubert M, Margerie P, Trap J, Bureau F. 2010. Aboveground-belowground relationships in temperate forests: Plant litter composes and microbiota orchestrates. *Forest Ecology and Management* **259**: 563--572.

Aubert M, Trap J, Chauvat M, Hedde M., Bureau F. 2018. Forest humus forms as a playground for studying aboveground-belowground relationships: Part 2, a case study along the dynamic of a broad lived plain forest ecosystem. *Applied Soil Ecology* **123**: 398--408.

Barré P, Plante A F, Cécillon L, Lutfalla S, Baudin F, Bernard S, Christensen B T, Eglin T, Fernandez J M, Houot S, Kätterer T, Le Guillou C, Macdonald A, van Oort F, Chenu C. 2016. The energetic and chemical signatures of persistent soil organic matter. *Biogeochemistry* **130**: 1--12.

Baudin F, Disnar J R, Aboussou A, Savignac F. 2015. Guidelines for Rock--Eval analysis of recent marine sediments. *Organic Geochemistry* **86**: 71--80.

Bätz N, Verrecchia E P, Lane S N. 2014. The role of soil in vegetated gravelly river braid plains: more than just a passive response? *Earth Surface Processes and Landforms* **40**: 143--156.

Behar F, Beaumont V, De B. Penteado H. 2001. Rock-Eval 6 technology: performances and developments. *Oil & Gas Science and Technology* **56**: 111--134.

Biester H, Knorr K H, Schellekens J, Basler A, Hermanns Y M. 2014. Comparison of different methods to determine the degree of peat decomposition in peat bogs. *Biogeosciences* **11**: 2691--2707.

Carrie J, Sanei H, Stern G. 2012. Standardisation of Rock–Eval pyrolysis for the analysis of recent sediments and soils. *Organic Geochemistry* **46**: 38--53.

Chauvat M, Bureau F, Perez G, Delporte P, Aubert M. 2011. Collembolan assemblages across a 130-year chronosequence of beech forest. *Soil organisms* **83**, 405--418.

Copard Y, Di-Giovanni C, Martaud T, Albéric P, Olivier J E. 2006. Using Rock-Eval 6 pyrolysis for tracking fossil organic carbon in modern environments: implications for the roles of erosion and weathering. *Earth Surface Processes and Landforms* **31**: 135--153.

Debret M, Bentaleb I, Sebag D, Favier C, Nguetsop V, Fontugne M, Oslisly R, Ngomanda A. 2014. Influence of inherited paleotopography and water level rise on the sedimentary infill of Lake Ossa (S Cameroon) inferred by continuous color and bulk organic matter analyses. *Palaeogeography, Palaeoclimatology, Palaeoecology* **411**: 110--121.

Delarue F, Disnar J R, Copard Y, Gogo S, Jacob J, Laggoun-Défarge F. 2013 Can Rock-Eval pyrolysis assess the biogeochemical composition of organic matter during peatification? *Organic Geochemistry* **61**: 66--72.

Di-Giovanni C, Disnar J R, Bichet V, Campy M. 1998. Meso-Cenozoic organic matter in present humus layers (Chaillexon basin, Doubs, France). *Comptes Rendus de l'Académie des Sciences, Série IIA* **326**: 553--559.

Disnar J R, Trichet J. 1984. The influence of various divalent cations (UO22+, Cu2+, Pb2+, Co2+, Ni2+, Zn2+, Mn2+) on the thermally induced evolution of organic matter isolated from an algal mat. *Organic geochemistry* **6**: 865--874.

Disnar J R, Guillet B, Keravis D, Di-Giovanni C, Sebag D. 2003. Soil organic matter (SOM) characterization by Rock-Eval pyrolysis: scope and limitations. *Organic Geochemistry* **34**: 327--343.

Espitalié J, Deroo G, Marquis F. 1985. Rock-Eval Pyrolysis and its applications. Part 1. *Revue de l'Institut français du Pétrole* **40**: 563--579.

Espitalié J, Laporte J L, Madec M, Marquis F, Leplat P, Paulet J, Boutefeu A. 1977. Méthode rapide de caractérisation des roches mètres, de leur potentiel pétrolier et de leur degré d'évolution. *Oil & Gas Science and Technology* **32**: 23--42.

Feller C, Brossard M, Chen Y, Landa E R, Trichet J. 2010. Selected Pioneering Works on humus in soils and sediments during the 20th century: a retrospective look from the International Humic Substances Society view. *Physics and Chemistry of the Earth*, **35**: 15--18.

Gillespie W, Sanei H, Diochon A, Ellert H, Regier Z, Chevrier D, Dynes J J, Tarnocai C, Gregorich E G. 2014. Perennially and annually frozen soil carbon differ in their susceptibility to decomposition: Analysis of Subarctic earth hummocks by bioassay, XANES and pyrolysis. *Soil Biology and Biochemistry* **68**: 106--116.

Graz Y, Di-Giovanni C, Copard Y, Elie M, Faure P, Laggoun Defarge F, Lévèque J, Michels R, Olivier J E. 2011. Occurrence of fossil organic matter in modern environments: Optical, geochemical and isotopic evidence. *Applied Geochemistry* **26**: 1302--1314.

Graz Y, Di-Giovanni C, Copard Y, Mathys N, Cras A, Marc V. 2012. Annual fossil organic carbon delivery due to mechanical and chemical weathering of marly badlands areas. *Earth Surface Processes and Landforms* **37**: 1263--1271.

Gregorich E G, Gillespie A W, Beare M H, Curtin D, Sanei H, Yanni S F. 2015. Evaluating biodegradability of soil organic matter by its thermal stability and chemical composition. *Soil Biology and Biochemistry* **91**: 182--191.

Hare A A, Kuzyk Z Z A, Macdonald R W, Sanei H, Barber D, Stern G A, Wang F. 2014. Characterization of sedimentary organic matter in recent marine sediments from Hudson Bay, Canada, by Rock-Eval pyrolysis. *Organic Geochemistry* **68**: 52--60.

Hedde M, Aubert M, Bureau F, Margerie P, Decaëns T. 2007. Soil detritivore macro-invertebrate assemblages throughout a managed beech rotation. *Annals of Forest Science* **64**: 219--228.

Hedde M, Aubert M, Decaëns T, Bureau F. 2008. Dynamics of soil carbon in a beechwood chronosequence forest. *Forest Ecology and Management* **255**: 193--202.

Hedde M, Bureau F, Chauvat M, Decaëns T. 2010. Patterns and mechanisms responsible for the relationship between the diversity of litter macro-invertebrates and leaf degradation. *Basic and Applied Ecology* **11**: 35--44.

Hermy M, Verheyen K. 2007. Legacies of the past in the present-day forest biodiversity: a review of past land-use effects on forest plant species composition and diversity. *Ecological Research* **22**: 361--371.

Hetényi M, Nyilas T, Tóth M. 2005. Stepwise Rock-Eval pyrolysis as a tool for typing heterogeneous organic matter in soils. *Journal of Analytical and Applied Pyrolysis* **74**: 45--54.

Jabiol B, Brêthes A, Ponge J F, Toutain F, Brun J J. 2007. L'humus sous toutes ses formes.

Katz, B.J. (1983) Limitations of Rock-Eval pyrolysis for typing organic matter. *Organic Geochemistry* **4**: 195--199.

Kruge M A, Mukhopadhyay P K, Lewis C F M. 1998. A molecular evaluation of contaminants and natural organic matter in bottom sediments from western Lake Ontario. *Organic geochemistry* **29**: 1797--1812.

Lafargue E, Marquis F, Pillot D. 1998. Rock-Eval 6 applications in hydrocarbon exploration, production, and soil contamination studies. *Oil & Gas Science and Technology* **53**: 421--437.

Lehmann J, Kleber M. 2015. The contentious nature of soil organic matter. *Nature* **528**: 60--68.

Malou O, Sebag D, Moulin P, Chevallier T, Badiane-Ndour N Y, Thiam A, Chapuis-Lardy L. 2020. The Rock-Eval® signature of soil organic carbon in arenosols of the Senegalese groundnut basin. How do agricultural practices matter? *Agriculture, Ecosystems and Environment* **300**: 107030.

Marchand C, Lallier-Vergès E, Disnar J R, Kéravis D. 2008. Organic carbon sources and transformations in mangrove sediments: A Rock-Eval pyrolysis approach. *Organic Geochemistry* **39**: 408--421.

Matteodo M, Grand S, Sebag D, Rowley M C, Vittoz P, Verrecchia E P. 2018. Decoupling of topsoil and subsoil controls on organic matter dynamics in the Swiss Alps. *Geoderma* **330**: 41--51.

Melenevskii V N, Leonova G A, Konyshev A S. 2011. The organic matter of the recent sediments of Lake Beloe (West Siberia). *Russian geology and geophysics* **52**: 583--592.

Newell A J, Vane C H, Sorensen J P, Moss-Hayes V, Gooddy D C. 2016. Long-term Holocene groundwater fluctuations in a chalk catchment: evidence from Rock-Eval pyrolysis of riparian peats. *Hydrological Processes* **30**: 4556--4567.

Noël H, Garbolino E, Brauer A, Lallier-Vergès E, de Beaulieu J L, Disnar J R. 2001. Human impact and soil erosion during the last 5000 yrs as recorded in lacustrine sedimentary organic matter at Lac d'Annecy, the French Alps. *Journal of Paleolimnology* **25**: 229--244.

Oen A M, Breedveld G D, Kalaitzidis S, Christanis K, Cornelissen G. 2006. How quality and quantity of organic matter affect polycyclic aromatic hydrocarbon desorption from Norwegian harbor sediments. *Environmental toxicology and chemistry* **25**: 1258--1267.

Pickett S T. 1989. Space-for-Time substitution as an alternative to long-term studies, In Likens G E (ed.) Long-Terme Studies in Ecology. Approaches and Alternatives. Springer-Verlag, pp. 110--135.

Poot A, Quik J T, Veld H, Koelmans A A. 2009. Quantification methods of Black Carbon: comparison of Rock-Eval analysis with traditional methods. *J Chromatogr A* **1216**: 613--622.

Saenger A, Cécillon L, Poulenard J, Bureau F, de Daniéli S, Gonzalez J M., Brun J J. 2015. Surveying the carbon pools of mountain soils: A comparison of physical fractionation and Rock-Eval pyrolysis. *Geoderma* **241-242**: 279--288.

Saenger A, Cécillon L, Sebag D, Brun J J. 2013. Soil organic carbon quantity, chemistry and thermal stability in a mountainous landscape: A Rock–Eval pyrolysis survey. *Organic Geochemistry* **54**: 101--114.

Schiedung M, Don A, Wordell-Dietrich P, Alcántara V, Kuner P, Guggenberger G. 2017. Thermal oxidation does not fractionate soil organic carbon with differing biological stabilities. *Journal of Plant Nutrition and Soil Science* **180**: 18--26.

Sebag D, Debret M, M'voubou Makaya, Mabicka Obame R, Ngomanda A., Oslisly R., Bentaleb I, Disnar J R, Giresse P. 2013. Coupled Rock-Eval pyrolysis and spectrophotometry for lacustrine sedimentary dynamics: Application for West Central African rainforests (Kamalete and Nguene lakes, Gabon). *The Holocene* **23**: 1173--1183.

Sebag D, Disnar J R, Guillet B, Di-Giovanni C, Verrecchia E P, Durand A. 2006. Monitoring organic matter dynamics in soil profiles by 'Rock-Eval pyrolysis': bulk characterization and quantification of degradation. *European Journal of Soil Science* **57**: 344--355.

Sebag D, Verrecchia E P, Cécillon L, Adatte T, Albrecht R, Aubert M, Bureau F, Cailleau G, Copard Y, Decaens T, Disnar J R, Hetényi M, Nyilas T, Trombino L. 2016. Dynamics of soil organic matter based on new Rock-Eval indices. *Geoderma* **284**: 185--203.

Six J, Paustian K, Elliott E T, Combrink C. 2000. Soil Structure and Organic Matter: I. Distribution of Aggregate-Size Classes and Aggregate-Associated Carbon. *Soil Science Society of America Journal* **64** (2), 681--689.

Six J, Conant R T, Paul E A, Paustian K. 2002. Stabilization Mechanisms of Soil Organic Matter: Implications for C-Saturation of Soils. *Plant and Soil* **241** (2) 155--176.

Steinmann P, Adatte T, Lambert P. 2003. Recent changes in sedimentary organic matter from Lake Neuchâtel (Switzerland) as traced by Rock-Eval pyrolysis. *Eclogae geol. Helv.* **96**: 109--116.

Tambach T J, Veld H, Griffioen J. 2009. Influence of HCl/HF treatment on organic matter in aquifer sediments: A Rock-Eval pyrolysis study. *Applied Geochemistry* **24**: 2144--2151.

Trap J, Bureau F, Akpa-Vinceslas M, Decaëns T, Aubert M. 2011a. Changes in humus forms and soil N pathways along a 130-yr-old pure beech forest chronosequence. *Ann. For. Sci.* **68**: 559--606.

Trap J, Bureau F, Brethes A, Jabiol B, Ponge J F, Chauvat M, Decaëns T, Aubert M. 2011b. Does moder development along a pure beech (Fagus sylvatica L.) chronosequence result from changes in litter production or in decomposition rates? *Soil Biology and Biochemistry* **43**: 1490--1497.

Trap J, Laval K, Akpa-Vinceslas M, Gangneux C, Bureau F, Decaëns T, Aubert M. 2011c. Humus macro-morphology and soil microbial community changes along a 130-yr-old Fagus sylvatica chronosequence. *Soil Biology and Biochemistry* **43**: 1553--1562.

Trap J, Bureau F, Perez G, Aubert M. 2013. PLS-regressions highlight litter quality as the major predictor of humus form shift along forest maturation. *Soil Biology and Biochemistry* **57**: 969--971.

Tyson R V. 1995. Sedimentary organic matter: organic facies and palynofacies. Chapman & Hall, London.

Von Lützow M, Kögel-Knabner I, Ekschmitt K, Flessa H, Guggenberger G, Matzner E, Marschner B. 2007. SOM Fractionation Methods: Relevance to Functional Pools and to Stabilization Mechanisms. *Soil Biology and Biochemistry* **39**: 2183--2207.

Zanella A, Ponge J F, Gobat J M, Juilleret J, Blouin M, Aubert M, Chertov O, Rubio J L, 2018. Humusica 1, article 1: Essential bases – Vocabulary. *Applied Soil Ecology* **122**: 10--21.

Table 1: Statistical values (1st quartile, median, 3rd quartile) of the measured and calculated Rock-Eval® parameters given in the text, for O and A horizons and their respective fraction sizes.

Type	**Typology**	**Grain size**	**TOC**	**TpS2**	**HI**	**OI**	**I**	**R**
All samples			9.7; **41.2** ; 50.2	372 ; **418** ; 458	276 ; **315** ; 394	77 ; **118** ; 188	0.13 ; **0.21** ; 0.39	0.42 ; **0.52** ; 0.57
Organic horizon								
OL horizon	*litter*	*bulk sample*	47.8 ; **48.7** ; 50.6	369 ; **371** ; 372	270 ; **287** ; 297	115 ; **119** ; 121	0.48 ; **0.49** ; 0.51	0.35 ; **0.36** ; 0.37
O-coarse fraction	*large debris*	*> 2000 µm*	44.4 ; **49.8** ; 53.6	370 ; **372** ; 375	249 ; **264** ; 273	111 ; **120** ; 159	0.36 ; **0.39** ; 0.42	0.40 ; **0.42** ; 0.44
O-medium fraction	*O-medium*	*2000 - 200 µm*	41.7 ; **50.1** ; 50.6	373 ; **374** ; 375	249 ; **267** ; 295	100 ; **111** ; 197	0.31 ; **0.34** ; 0.39	0.42 ; **0.46** ; 0.49
O-fine fraction	*O-fine*	*200 -50 µm*	34.6 ; **42.3** ; 48.9	366 ; **371** ; 373	294 ; **342** ; 378	69 ; **77** ; 236	0.35 ; **0.35** ; 0.36	0.43 ; **0.45** ; 0.46
Organo-mineral								
A horizon	*topsoil*	*bulk sample*	3.8 ; **4.6** ; 5.7	461 ; **463** ; 464	299 ; **312** ; 319	143 ; **144** ; 153	0.15 ; **0.17** ; 0.19	0.54 ; **0.55** ; 0.57
A-coarse fraction	*A-coarse*	*> 200 µm*	38.2 ; **48.6** ; 58.4	426 ; **432** ; 433	349 ; **382** ; 410	41 ; **50** ; 268	0.07 ; **0.09** ; 0.10	0.55 ; **0.57** ; 0.58
A-medium fraction	*A- medium*	*200 - 50 µm*	19.0 ; **24.4** ; 26.8	427 ; **437** ; 451	315 ; **370** ; 394	50 ; **63** ; 212	0.12 ; **0.15** ; 0.17	0.55 ; **0.57** ; 0.59
A-fine fraction	*A-fine*	*< 50 µm*	2.5 ; **3.2** ; 5.8	463 ; **464** ; 465	316 ; **338** ; 366	97 ; **151** ; 292	0.11 ; **0.12** ; 0.15	0.59 ; **0.60** ; 0.62

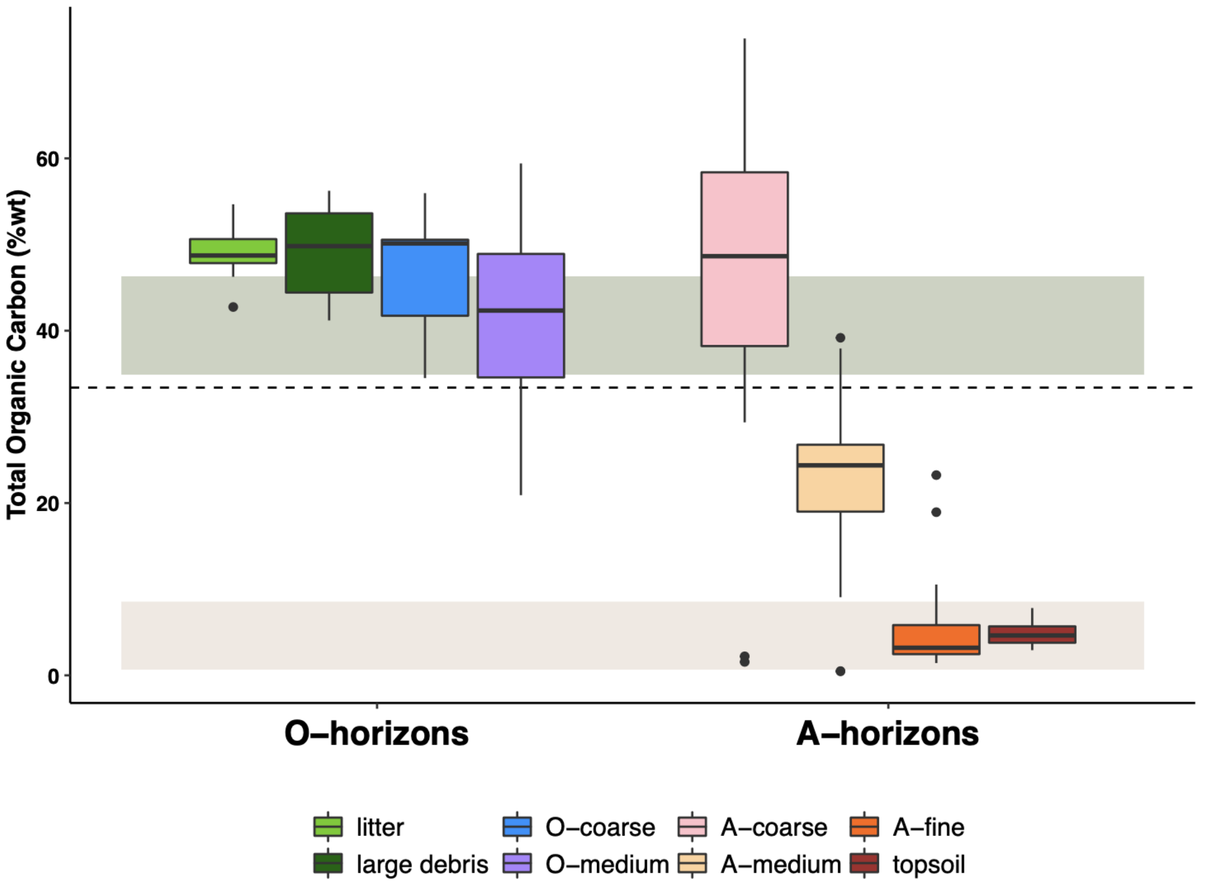

Fig. 1. Soil Organic Carbon (SOC %wt) contents of organic horizons (OL litters, OF/OH fractions) and organo-mineral horizons (A-fractions, A horizon). Horizontal bands highlight the range of values from Sebag *et al.* (2016)’s dataset for both bulk samples of litters (green) and topsoils (brown), respectively.

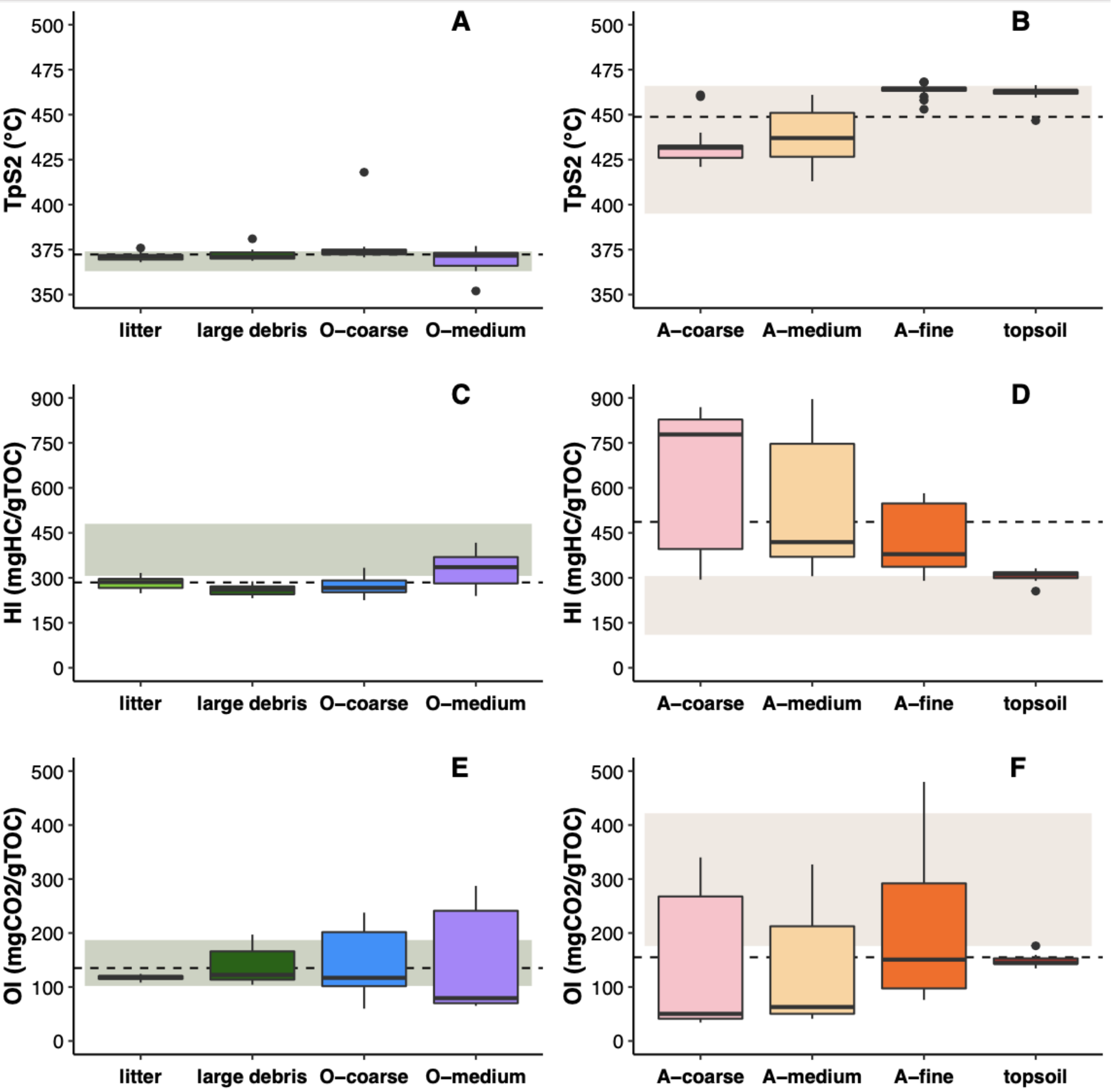

Fig. 2. Boxplots of standard Rock-Eval® parameters for the various fraction sizes: on the left-hand side, holorganic horizons (O); on the right-hand side, organo-mineral horizons (A). A-B. Temperatures corresponding to the maximum release of hydrocarbon effluents. C-D. Hydrogen Index (mg HC/g Corg). E-F Oxygen Index (mg CO_2/g Corg).

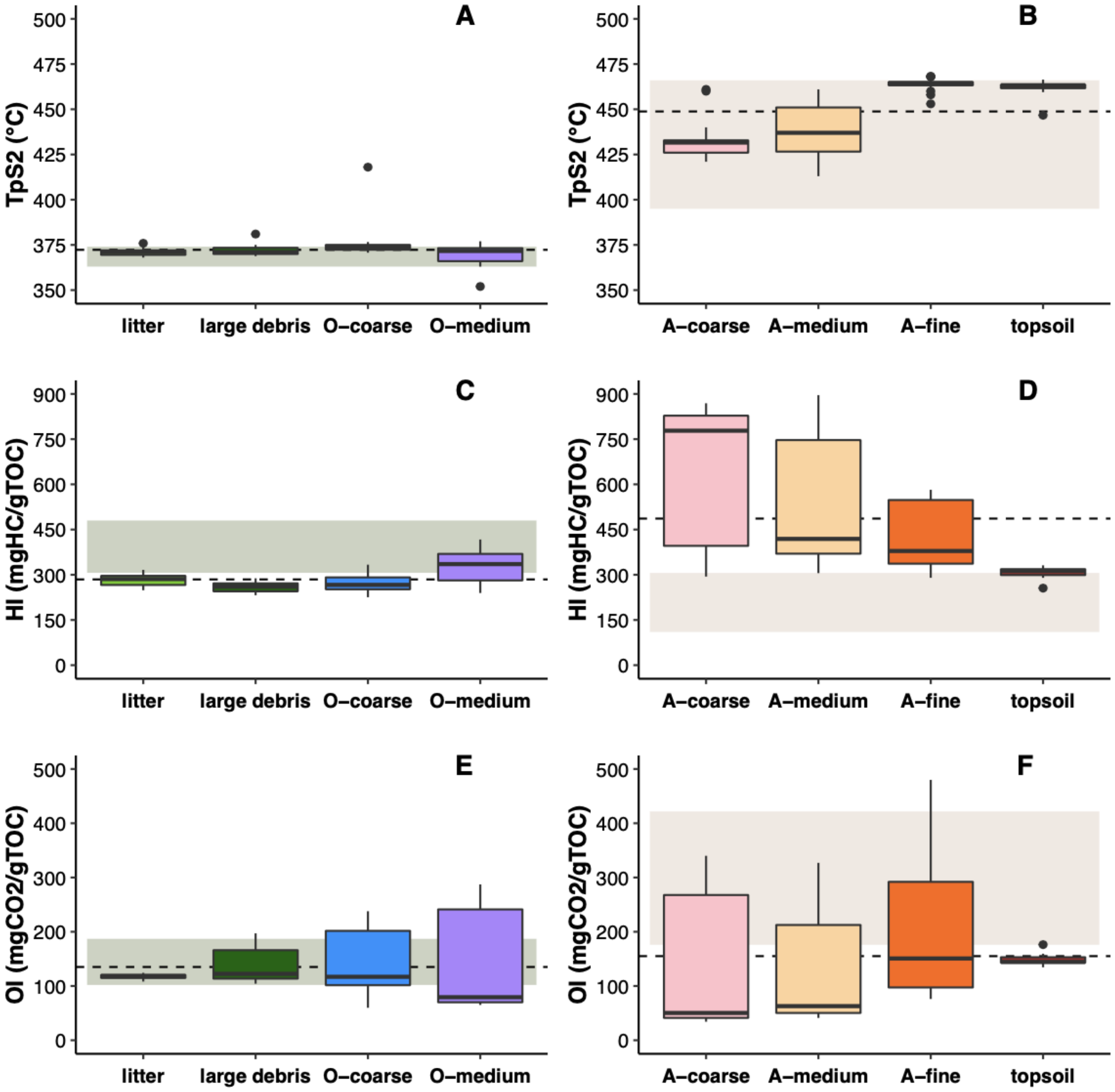

Fig. 3. SOC thermal stability (R-index) and preservation of thermolabile pool (I-index). A. I/R diagram for litters (OL), topsoil (A), and grain-size fractions. Horizontal bands highlight the range of values from Sebag *et al.* (2016)'s dataset for both bulk samples of litters (green) and topsoils (brown), respectively. The central regression line represents the "decomposition line" calculated using the Sebag *et al.* (2016)'s dataset (dotted line refers to the 95% confidence interval). The two other regressions refer to the A-coarse fraction (bottom lines) and the A-fine fraction (upper lines). B. Range of R-index values for A-fractions and topsoil. C. Range of I-index values for A-fractions and topsoil.

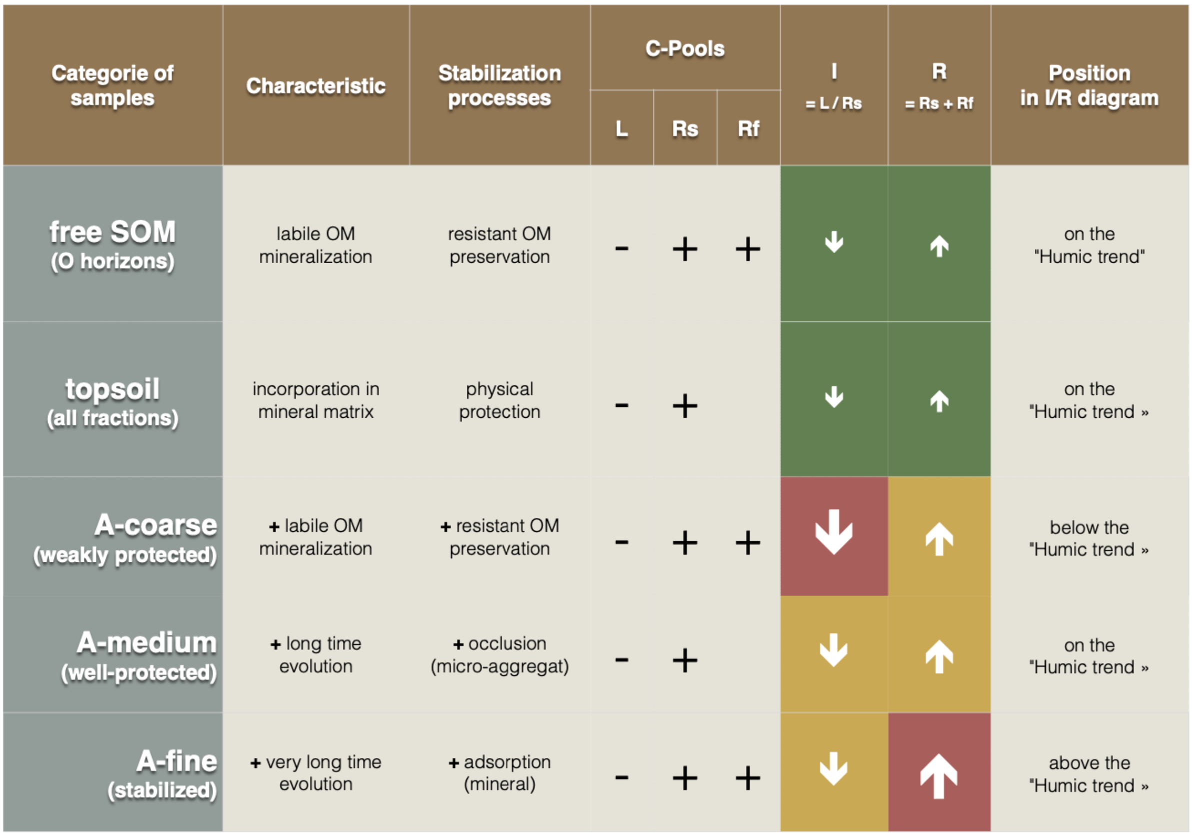

Categorie of samples	Characteristic	Stabilization processes	C-Pools			I	R	Position in I/R diagram
			L	Rs	Rf	= L / Rs	= Rs + Rf	
free SOM (O horizons)	labile OM mineralization	resistant OM preservation	-	+	+	↓	↑	on the "Humic trend"
topsoil (all fractions)	incorporation in mineral matrix	physical protection	-	+		↓	↑	on the "Humic trend »
A-coarse (weakly protected)	+ labile OM mineralization	+ resistant OM preservation	-	+	+	↓	↑	below the "Humic trend »
A-medium (well-protected)	+ long time evolution	+ occlusion (micro-aggregat)	-	+		↓	↑	on the "Humic trend »
A-fine (stabilized)	+ very long time evolution	+ adsorption (mineral)	-	+	+	↓	↑	above the "Humic trend »

Fig. 4. Key for I/R diagram interpretation from relationships between thermal stability indices, size fractions, C-pools (labile, resistant, refractory), and some pedogenic processes. L: thermo-labile C pools; Rs: thermo-resistant C-pool; Rf: thermo-refractory C-pool. I : I-index; R: R-index. Colors and arrow sizes refer to the effect of the stabilization process on the indices: decreasing of I-index and concomitant increasing R-index. If the two changes are equivalent, data plot on the "decomposition line"; if the decreasing is higher than the increasing, then data plot below the "decomposition line"; finally, if the increasing is higher than the decreasing, then data plot above the "decomposition line".

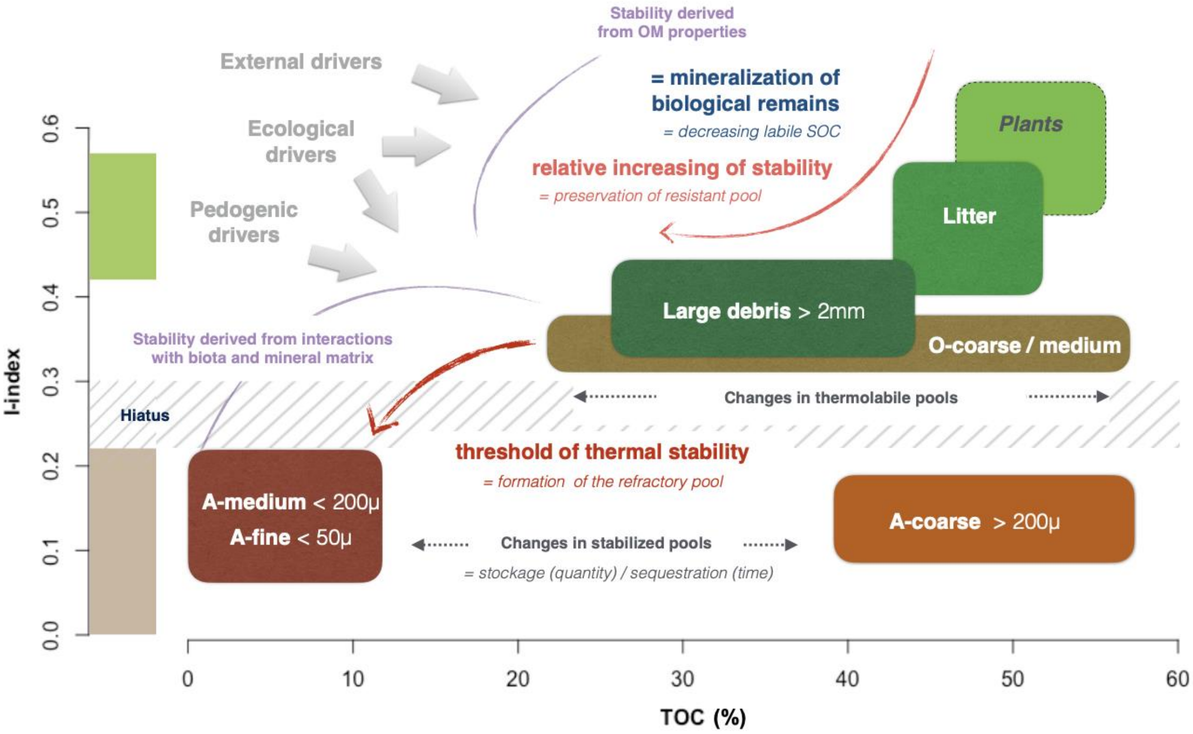

Fig. 5. Changes in soil organic carbon quantity (TOC in g C per 100g of sample) compared to SOM quality (I-index as a degree of preservation of the thermolabile pool) according the grain-size fractions in relationship with external drivers, biota, and mineral matrix. In the various fractions of O-horizons, the main factor is a mineralization (decreasing TOC) of biological compounds, leading to relative increasing of SOM stability (decreasing I-index) due to preservation of a resistant pool. In the fractions of the A-horizons, stability derives from the interaction between biota and mineral matrix leading to a higher SOM stability (gap in the I-index) due to the formation of a refractory pool. This change in stability can induce an increase in TOC as a result of sequestration.

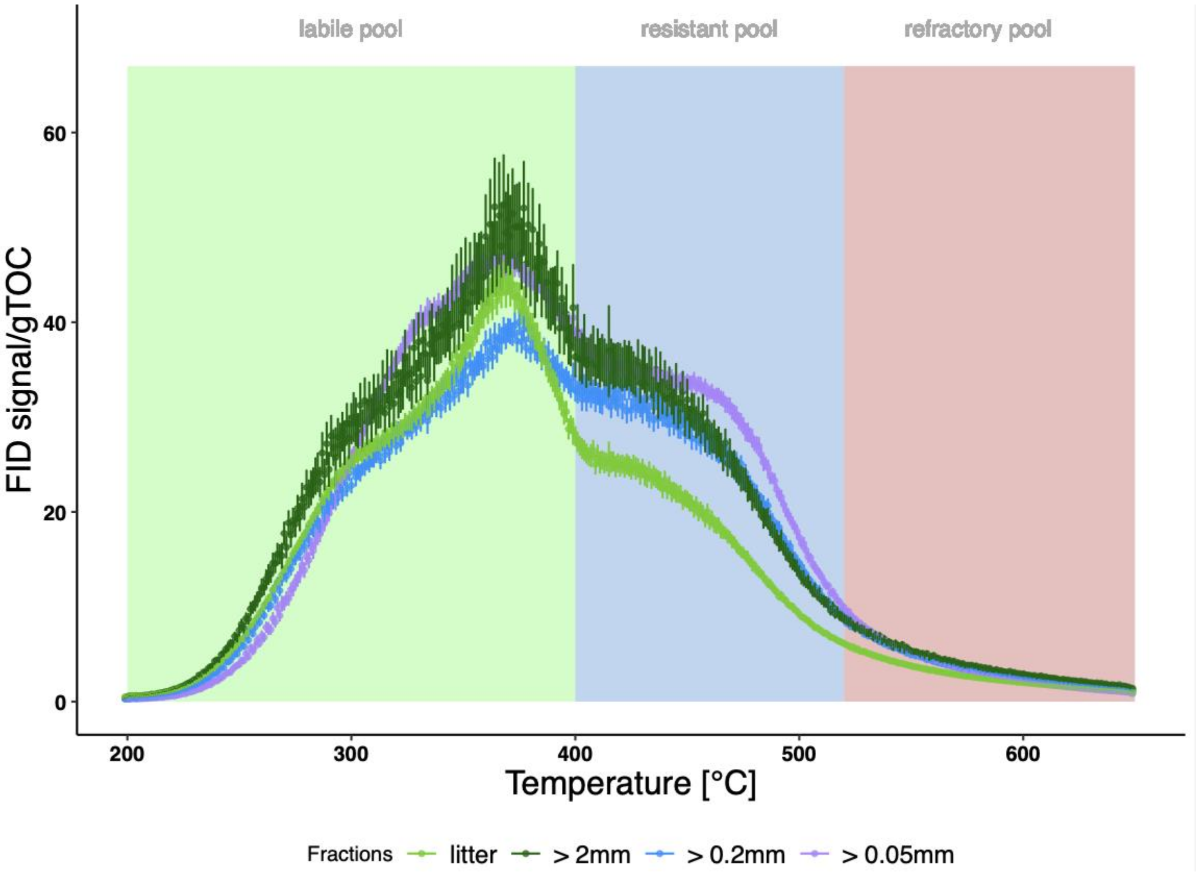

SM1. Average S2 thermograms and associated standard error for organic layers and O-fractions. The area below each curve corresponds to the total HC amount (with respect to an equivalent organic C content) released during the pyrolysis phase.

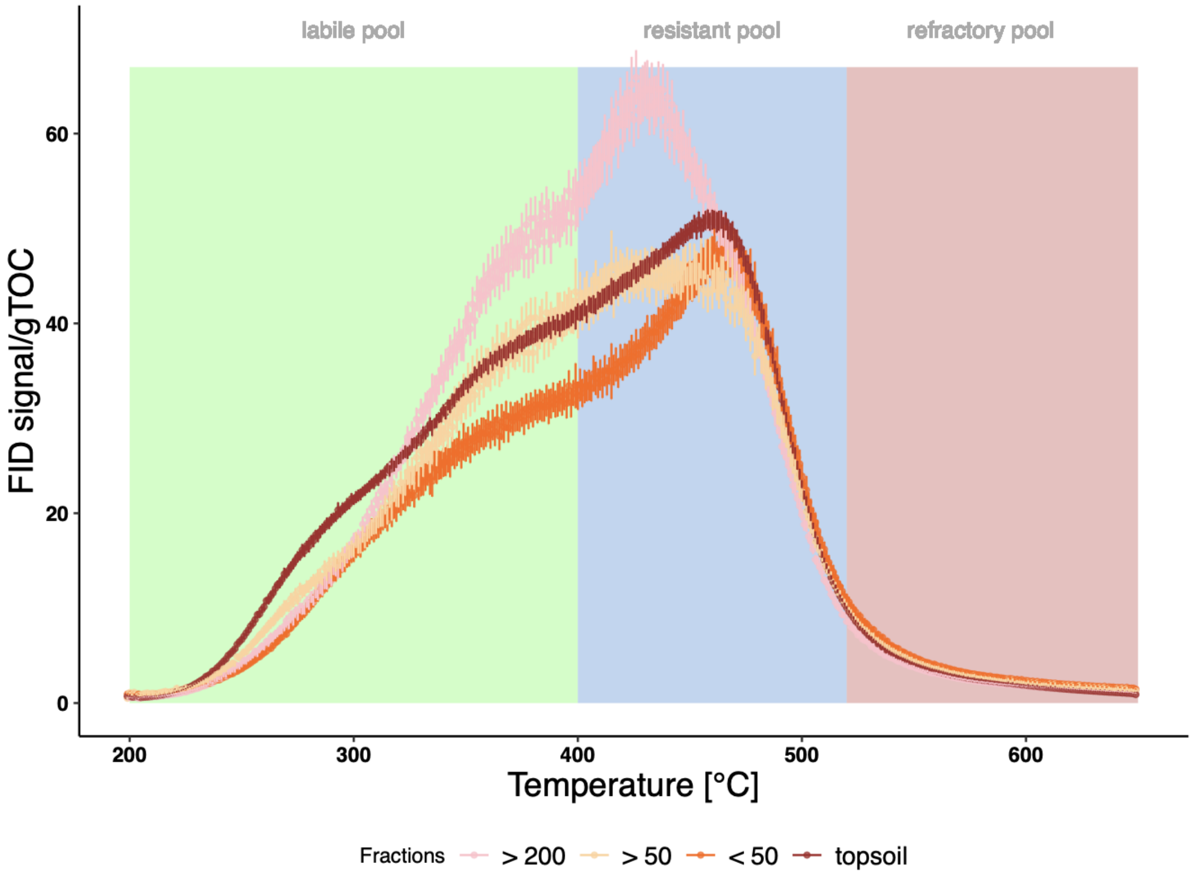

SM2. Average S2 thermograms and associated standard error for topsoils and A-fractions. The area below each curve corresponds to the total HC amount (with respect to an equivalent organic C content) released during the pyrolysis phase.